The $K^- p \to \eta\Lambda$ reaction in an effective Lagrangian model

Bo-Chao Liu[1,*] and Ju-Jun Xie[2,3,†]

[1]*Department of Applied Physics, Xi'an Jiaotong University, Xi'an, Shanxi 710049, China*
[2]*Department of Physics, Zhengzhou University, Zhengzhou, Henan 450001, China*
[3]*Instituto de Física Corpuscular (IFIC), Centro Mixto CSIC-Universidad de Valencia, Institutos de Investigación de Paterna,*
Apartado Postal 22085, E-46071 Valencia, Spain

We report on a theoretical study of the $K^- p \to \eta\Lambda$ reaction near threshold by using an effective Lagrangian approach. The role of s-channel $\Lambda(1670)$, t-channel K^*, and u-channel proton pole diagrams are considered. We show that the total cross section data are well reproduced. However, only including the s-wave $\Lambda(1670)$ state and the background contribution from t and u channels is not enough to describe the bowl structures in the angular distribution of the $K^- p \to \eta\Lambda$ reaction, which indicates that there should be higher partial waves contributing to this reaction in some energy region. Indeed, if we considered the contributions from a D_{03} resonance, we could describe the bowl structures; however, a rather small width (~ 2 MeV) of this resonance would be needed.

The K^--induced reactions are an important tool to gain a deeper understanding of the $\bar{K}N$ interactions and also of the nature of the hyperon resonance. The reaction $K^- p \to \eta\Lambda$ is of particular interest in the hyperon resonances since there are no isospin-1 hyperons contributing here and it gives us a rather clear channel to study the Λ resonances. Ten years ago, the differential and total cross sections of the $K^- p \to \eta\Lambda$ reaction were measured, with much higher precision than previous measurements, by the Crystal Ball Collaboration [1]. These new data were obtained with a beam momentum of K^- from threshold to 770 MeV/c, corresponding to invariant mass $\sqrt{s} = 1.664$–1.685 GeV.

Current knowledge of Λ resonances are mainly known from the analysis of $\bar{K}N$ reactions in the 1970s, and large uncertainties exist because of poor statistics of data and limited knowledge of background contributions [2,3]. Besides, the nature of some Λ states are still controversial. Based on the available new data with much higher precision, the authors of Ref. [1] came to the conclusion that $\Lambda(1670)$ should be a three-quark state, while on the contrary the authors of Refs. [4,5] argued that $\Lambda(1670)$ is a dynamically generated state. On the other hand, the traditional three-quark features of $\Lambda(1670)$ are shown in Ref. [6] from a study of the $K^- p \to \pi^0\Sigma^0$ reaction at low energies by using a chiral quark model. It is clear that some further and detailed studies, on both the theoretical and the experimental sides, are still necessary.

Because the $\Lambda(1670)$ state has a large coupling to the $\bar{K}N$ and $\eta\Lambda$ channels, it is expected that Λ^* should dominate this reaction near threshold. In the present work, we reanalyze the $K^- p \to \eta\Lambda$ reaction near threshold within the effective Lagrangian method. In addition to the main contribution from the $\Lambda(1670)$ state, the "background" contributions from the t-channel K^* exchange and the u-channel proton exchange are also studied.

The basic Feynman diagrams are shown in Fig. 1. These include the t-channel K^* exchange, the u-channel proton exchange, and the s-channel $\Lambda(1670)(\equiv \Lambda^*)$ terms. To compute the contributions of these terms, we use the interaction Lagrangian densities of Refs. [7–10]:

$$\mathcal{L}_{K^*K\eta} = g_{K^*K\eta}(\eta\partial^\mu K^- - K^-\partial^\mu\eta)K_\mu^{*-}, \tag{1}$$

$$\mathcal{L}_{K^*N\Lambda} = g_{K^*N\Lambda}\bar{\Lambda}\left(\gamma_\mu - \frac{\kappa}{2M_N}\sigma_{\mu\nu}\partial^\nu\right)K^{*\mu}N + \text{H.c.}, \tag{2}$$

$$\mathcal{L}_{\eta NN} = g_{\eta NN}\bar{N}\gamma_5 N\eta, \tag{3}$$

$$\mathcal{L}_{KN\Lambda} = g_{KN\Lambda}\bar{N}\gamma_5\Lambda K + \text{H.c.}, \tag{4}$$

$$\mathcal{L}_{\Lambda^*\bar{K}N} = g_{\Lambda^*\bar{K}N}\bar{\Lambda}^*\bar{K}N + \text{H.c.}, \tag{5}$$

$$\mathcal{L}_{\Lambda^*\Lambda\eta} = g_{\Lambda^*\Lambda\eta}\bar{\Lambda}^*\eta\Lambda + \text{H.c.}, \tag{6}$$

where we take $\kappa = 2.43$, which has been determined by the Nijmegen potential [11] and has been used in Ref. [12]. Other coupling constants are discussed below.

With the effective Lagrangian densities given above, we can easily construct the invariant scattering amplitudes:

$$\mathcal{M}_i = \bar{u}_{r_2}(p_4)\mathcal{A}_i u_{r_1}(p_2), \tag{7}$$

where i denotes the ith channel that contributes to the total amplitude, and $\bar{u}_{r_2}(p_4)$ and $u_{r_1}(p_2)$ are the spinors of Λ and proton, respectively. The reduced $\mathcal{A}_i$ read

$$\mathcal{A}_s = g_{\Lambda^*\bar{K}N}g_{\Lambda^*\Lambda\eta}\frac{\not{p}_1 + \not{p}_2 + M_{\Lambda^*}}{s - M_{\Lambda^*}^2 + iM_{\Lambda^*}\Gamma_{\Lambda^*}}, \tag{8}$$

$$\mathcal{A}_t = i\frac{g_{K^*K\eta}g_{K^*\Lambda N}}{q^2 - m_{K^*}^2}\left(\not{p}_1 + \not{p}_3 - \frac{m_K^2 - m_\eta^2}{m_{K^*}^2}\not{q}\right.$$
$$\left. - \frac{\kappa}{m_N}(p_1 p_3 - \not{p}_1\not{p}_3)\right), \tag{9}$$

$$\mathcal{A}_u = -g_{K\Lambda N}g_{\eta NN}\frac{\not{p}_2 - \not{p}_3 - m_N}{u - m_N^2}, \tag{10}$$
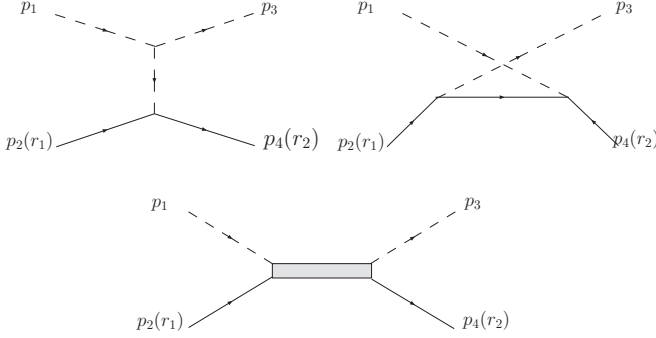
*liubc@xjtu.edu.cn
†xiejujun@mail.ihep.ac.cn

FIG. 1. Model for the reaction $K^- p \to \eta \Lambda$. In these diagrams, we show the definition of the kinematical (p_1, p_2, p_3, p_4) and polarization (r_1, r_2) variables that we use in our calculation.

where q is the momentum of exchanging meson K^* in the t channel. The width of K^* is not taken into account because K^* is in the t channel. The subindices s, t, and u stand for the s-channel Λ^* exchange, the t-channel K^* exchange, and the u-channel proton pole terms. As we can see, in the tree-level approximation, only the products like $g_{\Lambda^* \bar{K} N} g_{\Lambda^* \Lambda \eta}$ enter in the invariant amplitudes. They are determined with the use of MINUIT, by fitting to the experimental data [1], including the total and differential cross sections. Besides, M_{Λ^*} and Γ_{Λ^*} are the mass and the total decay width of the Λ^* resonance, which are free parameters in the present work and will be also fitted to the experimental data.

Because we are not dealing with pointlike particles, we ought to introduce the compositeness of the hadrons. This is usually achieved by including form factors in the amplitudes. In the present work, we adopt the following form factors [7,9,10]:

$$F\left(q_{\rm ex}^2, M_{\rm ex}\right) = \frac{\Lambda^4}{\Lambda^4 + \left(q_{\rm ex}^2 - M_{\rm ex}^2\right)^2}, \qquad (11)$$

for the s and u channels, and

$$F(q_{ex}^2, M_{ex}) = \left(\frac{\Lambda^2 - M_{ex}^2}{\Lambda^2 - q_{ex}^2}\right)^2, \qquad (12)$$

for t-channel, where the q_{ex} and M_{ex} are the four-momenta and the mass of the exchanged hadron, respectively. For the cutoff parameters, we take $\Lambda = 2.0$ GeV for the s channel and $\Lambda = 1.5$ GeV for the t and u channels.

The differential cross section for $K^- p \to \eta \Lambda$ at center of mass (c.m.) frame can be expressed as

$$\frac{d\sigma}{d\cos\theta_{\rm c.m.}} = \frac{1}{32\pi s} \frac{|\vec{p}_3^{\rm\ c.m.}|}{|\vec{p}_1^{\rm\ c.m.}|} \left(\frac{1}{2} \sum_{r_1, r_2} |\mathcal{M}|^2\right), \qquad (13)$$

where $\theta_{\rm c.m.}$ denotes the angle of the outgoing η relative to the beam direction in the c.m. frame, and $s = (p_1 + p_2)^2$ is the invariant mass square of the system.

In Eq. (13), the total invariant scattering amplitude $\mathcal{M}$ is given by

$$\mathcal{M} = \mathcal{M}_s + e^{i\theta_1} \mathcal{M}_t + e^{i\theta_2} \mathcal{M}_u. \qquad (14)$$

TABLE I. Adjusted parameters for the $\Lambda(1670)$ resonance. PDG estimates are also listed for comparison.

	Mass (MeV)	$\Gamma_{\rm tot}$ (MeV)	$|g_{\Lambda^* \bar{K} N} g_{\Lambda^* \eta \Lambda}|$
This calculation	1671.5 ± 0.2	23.3 ± 0.2	0.28 ± 0.03
PDG	$1660 \sim 1680$	$25 \sim 50$	0.31 ± 0.15

In the phenomenological Lagrangian approaches, the relative phases between amplitudes from different diagrams are not fixed, so we introduce two relative phases θ_1 and θ_2 between the background and the Λ^* contributions as free parameters, which will be determined by fitting to the experimental data.

We perform a seven-parameter (M_{Λ^*}, Γ_{Λ^*}, $g_{\Lambda^* \bar{K} N} g_{\Lambda^* \Lambda \eta}$, $g_{K^* N \Lambda} g_{K^* K \eta}$, $g_{K N \Lambda} g_{\eta N N}$, θ_1, and θ_2) χ^2 fit to the total and differential cross section data taken from Ref. [1]. There is a total of 155 data points. The fitted parameters for $\Lambda(1670)$ are shown in Table I and other fitted results are $g_{K^* N \Lambda} g_{K^* K \eta} = 14.8 \pm 1.7$, $g_{K N \Lambda} g_{\eta N N} = -5.6 \pm 0.9$, $\theta_1 = 2.9 \pm 0.2$, and $\theta_2 = 2.9 \pm 0.3$. The resultant χ^2/dof is 1.3.

On the other hand, the coupling constants of $g_{\Lambda^* \bar{K} N}$ and $g_{\Lambda^* \eta \Lambda}$ can be also evaluated from the $\Lambda(1670)$ resonance to $\bar{K} N$ and $\eta \Lambda$ partial decay widths:

$$\Gamma_{\Lambda^* \to \bar{K} N} = \frac{g_{\Lambda^* \bar{K} N}^2}{2\pi} (E_N + m_N) \frac{|\vec{p}_N|}{M_{\Lambda^*}}, \qquad (15)$$

$$\Gamma_{\Lambda^* \to \eta \Lambda} = \frac{g_{\Lambda^* \eta \Lambda}^2}{4\pi} (E_\Lambda + m_\Lambda) \frac{|\vec{p}_\Lambda|}{M_{\Lambda^*}}, \qquad (16)$$

where

$$E_{N/\Lambda} = \frac{M_{\Lambda^*}^2 + m_{N/\Lambda}^2 - m_{\bar{K}/\eta}^2}{2M_{\Lambda^*}}, \qquad (17)$$

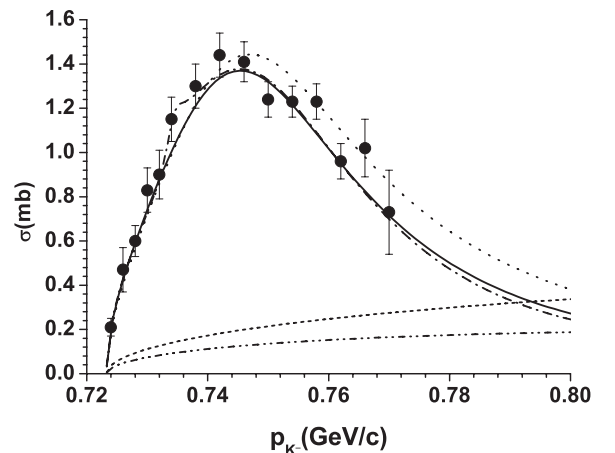$$|\vec{p}_{N/\Lambda}| = \sqrt{E_{N/\Lambda}^2 - m_{N/\Lambda}^2}. \qquad (18)$$

FIG. 2. $K^- p \to \eta \Lambda$ total cross sections compared with the data [1]. Results have been obtained from the best χ^2 fit. The solid line represents the full results, while the contribution from $\Lambda(1670)$, t-channel, and u-channel diagrams are shown by the dotted, dashed, and dot-dot-dashed lines, respectively. The dot-dashed line represents the best results for the total cross sections after including the D_{03} state.

With the value of total decay width $\Gamma_{\Lambda^*} = 35 \pm 15$ MeV, a value of 0.25 ± 0.05 for the $\Lambda^* \to \bar{K}N$ branching ratio, and a value of 0.175 ± 0.075 for the $\Lambda^* \to \eta\Lambda$ branching ratio, quoted in the Particle Data Group (PDG) book [2], we can get $|g_{\Lambda^*\bar{K}N}g_{\Lambda^*\eta\Lambda}| = 0.31 \pm 0.15$, which is also shown in Table I for comparison. The error ± 0.15 came from the errors of the $\Lambda^* \to \bar{K}N$ and $\Lambda^* \to \eta\Lambda$ partial decay widths.

As we can see in Table I, the fitted parameters for the $\Lambda(1670)$ resonance agree well with those of the PDG estimation. During the best fit, we adjusted the product of the coupling constants to experimental data. If we take $g_{K^*K\eta} = 1.6$ that was obtained from the SU(3) prediction [7], then we can get $|g_{K^*N\Lambda}| = 9.3 \pm 1.0$, which roughly agrees with the value $|g_{K^*N\Lambda}| = 6.1$, which was obtained from the SU(3) flavor symmetry in Ref. [11]. Because the value of $g_{\eta NN}$ is extremely uncertain and if we adopt it as 2.24, which was used in Ref. [8], then we get $|g_{KN\Lambda}| = 2.5 \pm 0.5$, which is much different with the SU(3) prediction value 13.3 [13,14]. However, as we mentioned above, the uncertainty of $g_{\eta NN}$

is very large [15–20], so the adjusted coupling constant $g_{KN\Lambda}$, in the present work, may be still within the SU(3) prediction.

Our best fits to the experimental data of the total cross sections are shown in Fig. 2, comparing with the data. The solid line represents the full results, while the contributions from the $\Lambda(1670)$, t-channel, and u-channel diagrams are shown by the dotted, dashed, and dot-dot-dashed lines, respectively. From Fig. 2, one can see that we can describe the data of total cross sections quite well and the $\Lambda(1670)$ resonance gives the dominant contribution, while the t- and u-channel diagrams give minor but sizable contributions.

The results of the best fit for the differential cross sections are shown by the solid line in Fig. 3. From there we can see that the deviations between our theoretical results and experimental data are evident especially for the angular distribution at $p_{K^-} = 730, 732, 734, 738$, and 742 MeV, where bowl-shaped structures in angular dependence appear. It also should be noted that, with including the background contribution from
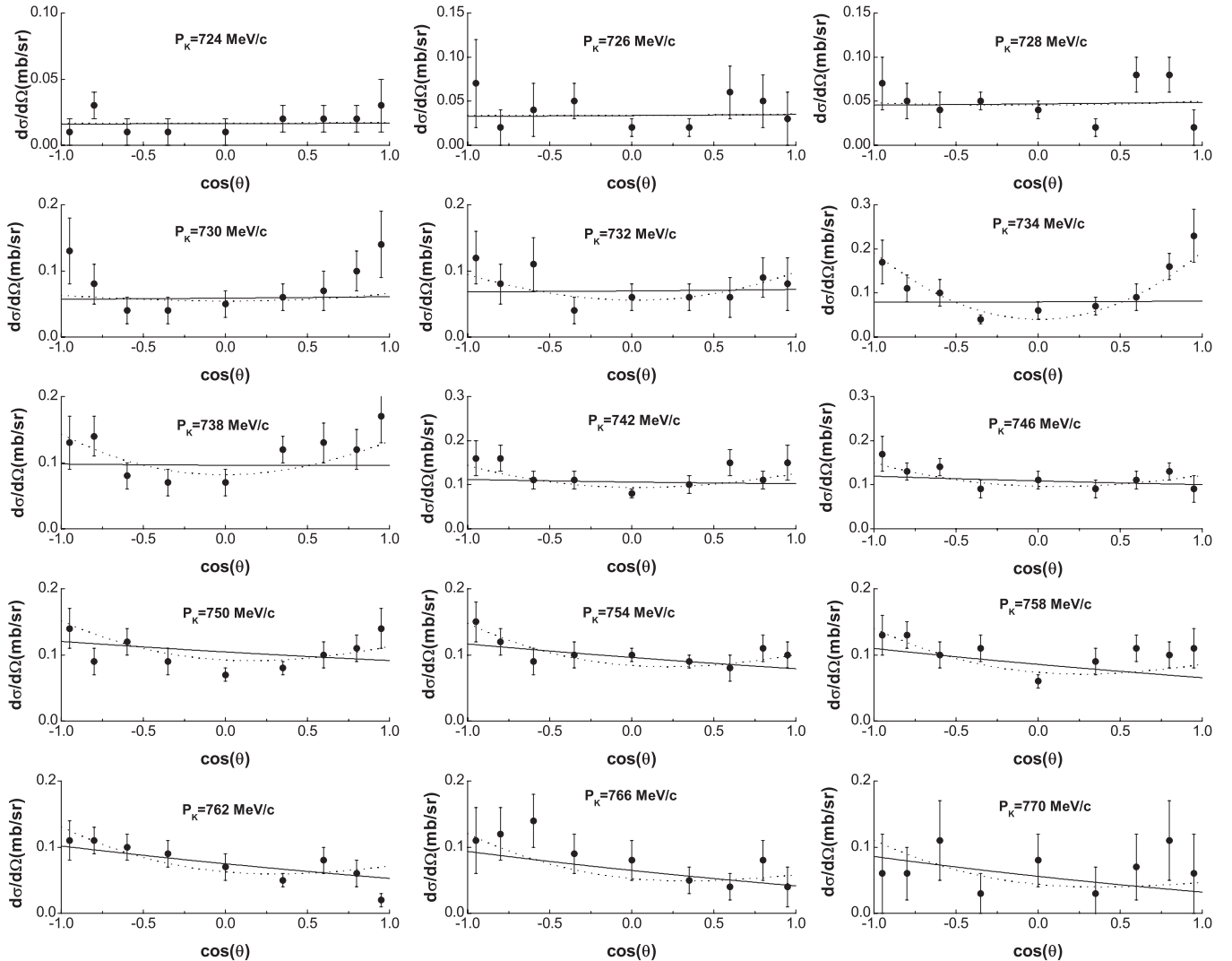

FIG. 3. The best-fitting results for differential cross sections. The solid lines represent the results by considering only $\Lambda(1670)$ and background contributions, while the dashed lines represent the results by including also a narrow D_{03} resonance.

the t-channel K^* exchange and the u-channel proton exchange, the backward enhancement in the angular distribution for p_{K^-} from 750 to 770 MeV is reproduced.

In order to obtain a better description of the differential cross section data, especially at some energy points, some other resonances that may contribute to this reaction should also be considered. For the bowl structures in differential cross sections, one possible explanation is that there might be d-wave contributions from the s channel with the excitation of the D_{03} resonance. For checking this, we performed another best fit: in addition to the contributions that were already considered in the previous fit, the contribution from the D_{03} state in the s-channel process is also included. The new best fitting gives $\chi^2/dof = 0.9$ and we get a satisfied description for both total cross sections and differential cross sections. The new results for the total cross sections are similar to the previous results except for a small bump around $p_{K^-} = 736$ MeV(see the dot-dashed line in Fig. 2). The corresponding results for differential cross sections are shown by the dotted line in Fig. 3, where the bowl structures are well reproduced.

The fitted parameters for the D_{03} resonance are mass $M = 1668.5 \pm 0.5$ MeV and the total decay width $\Gamma = 1.5 \pm 0.5$ MeV. The mass of D_{03} is close to the PDG estimate for $\Lambda(1690)$ ($M_{\Lambda(1690)} = 1690 \pm 5$ MeV), while the width is too small compared to the PDG estimate ($\Gamma_{\Lambda(1690)} = 60 \pm 10$ MeV). The width obtained from the best fit is narrow because the bowl structures in the differential cross sections show up in a narrow (± 3 MeV)[1] energy window.

One might think that releasing the limit of the cutoff values for the form factors and including more Λ resonances [such as] might improve the situation where the width of the D_{03}

state is too narrow. We have explored such a possibility, but we have found tiny changes. The new best fit still favors a D_{03} resonance with a very small width and the corresponding values for the parameters of a D_{03} resonance are close to the values that were obtained above.

In summary, we have studied the $K^- p \to \eta \Lambda$ reaction near threshold by using an effective Lagrangian approach. The role of the s-channel $\Lambda(1670)$, t-channel K^* and u-channel proton pole diagrams are considered. The total cross section is well reproduced. Our results show that the $\Lambda(1670)$ resonance gives the dominant contribution, while the t- and u-channel diagrams give minor but sizable contributions, especially for the backward enhancement in the angular distribution for p_{K^-} from 750 to 770 MeV.

However, including the $\Lambda(1670)$ resonance in the s-channel as well as the background contributions is not enough to describe the bowl structures in the angle distributions at some beam momentum points. A general opinion is that these bowl structures in angular distribution can be understood by further including the contribution from $\Lambda(1690)D_{03}$. Indeed, our calculations show that, with considering the D_{03} resonance, we can describe the bowl structures, but a rather small width of this resonance is needed. This means that the experimental data cannot be understood by considering the conventional $\Lambda(1690)$ resonance. On the other hand, the current experimental data still have systematic uncertainties especially when we look at the angular distribution data obtained from two different ways of identifying the final η meson (see Fig. 20 of Ref. [1]), so the present results give a signal for the need for further studies of this reaction.

---

[1]This is evaluated from the $K^- p$ invariant mass changed, with the range 730–742 MeV of p_{K^-}, by using the relation $s = (p_1 + p_2)^2 = m_{K^-}^2 + m_p^2 + 2m_p\sqrt{m_{K^-}^2 + p_{K^-}^2}$.

---

[1] A. Starostin *et al.*, Phys. Rev. C **64**, 055205 (2001).

[2] K. Nakamura *et al.*, J. Phys. G **37**, 075021 (2010).

[3] P. Z. Gao, B. S. Zou, and A. Sibirtsev, Nucl. Phys. A **867**, 41 (2011).

[4] E. Oset, A. Ramos, and C. Bennhold, Phys. Lett. B **527**, 99 (2002).

[5] T. Schafer, Phys. Rev. D **66**, 076009 (2002).

[6] Xian-Hui Zhong and Qiang Zhao, Phys. Rev. C **79**, 045202 (2009).

[7] F. Q. Wu, B. S. Zou, L. Li, and D. V. Bugg, Nucl. Phys. A **735**, 111 (2004); F. Q. Wu and B. S. Zou, Phys. Rev. D **73**, 114008 (2006).

[8] J. J. Xie, B. S. Zou, and H. C. Chiang, Phys. Rev. C **77**, 015206 (2008).

[9] G. Penner and U. Mosel, Phys. Rev. C **66**, 055211 (2002); **66**, 055212 (2002); V. Shklyar, H. Lenske, and U. Mosel, *ibid.* **72**, 015210 (2005).

[10] T. Feuster and U. Mosel, Phys. Rev. C **58**, 457 (1998); **59**, 460 (1999).

[11] V. G. J. Stoks and Th. A. Rijken, Phys. Rev. C **59**, 3009 (1999).

[12] Y. Oh and H. Kim, Phys. Rev. C **73**, 065202 (2006).

[13] Y. Oh, K. Nakayama, and T. S. H. Lee, Phys. Rep. **423**, 49 (2006).

[14] Y. Oh, C. M. Ko, and K. Nakayama, Phys. Rev. C **77**, 045204 (2008).

[15] W. Grein and P. Kroll, Nucl. Phys. A **338**, 332 (1980).

[16] M. Kirchbach and L. Tiator, Nucl. Phys. A **604**, 385 (1996).

[17] S. L. Zhu, Phys. Rev. C **61**, 065205 (2000).

[18] G. Faldt and C. Wilkin, Phys. Scr. **64**, 427 (2001).

[19] L. Tiator, C. Bennhold, and S. S. Kamalov, Nucl. Phys. A **580**, 455 (1994).

[20] K. Nakayama, Y. Oh, and H. Haberzettl, J. Korean Phys. Soc. **59**, 224 (2011).